2022

Comparison of Peak Skin Dose Calculated by Patient Radiation Dose Monitoring and Tracking Systems versus Solid-State Detector Measurements

Vincent D. Gargaro
Virginia Commonwealth University

Comparison of Peak Skin Dose Calculated by Patient Radiation Dose Monitoring and Tracking Systems versus Solid-State Detector Measurements

A thesis submitted in partial fulfillment of the requirements for the degree of Master of Science at Virginia Commonwealth University

By

Vincent Gargaro

Bachelor of Science in Biomedical Physics, University of Toledo, May 2020

Advisor: Frank D. Crowin, Ph.D.

Associate Professor

Department of Radiation Oncology

Virginia Commonwealth University

Richmond, VA

April 13th, 2022

Acknowledgments

First off, I would like to thank my parents, Vince and Linda. Without your support, I would not be where I am today. Dad, thank you for being a lifelong mentor. You have made me into the man, and Medical Physicist I am today. I am forever grateful for the knowledge of this field you have given me. Also, I would like to thank my girlfriend, Samantha. Your continued encouragement pushed me to the very end. Next, I would like to thank my sisters, Nicole, and Amanda, along with my brother-in-law Danny. Your ability to listen and guide me through every stressful situation did not go unappreciated. Finally, to my advisory committee, especially Dr. Frank Corwin, for guiding me along this process and making it all possible. To the VCU faculty, I thank you for your continued support and assistance throughout my time as a Ram.

Table of Contents

Figures

Equations

Tables

Graphs

Abbreviations

Abbreviations:	Term:	Units:
A_{skin}	Projected x-ray field size on patient	Centimeters squared (cm^2)
BSF	Backscatter Factor	--
C_x	Position of Collimator	Pixels
ESAK	Entrance Skin Air Kerma	Gray (Gy)
f	f-factor	Gray per Roentgen (Gy/R)
FOV	Field of View	Centimeters (cm)
FPD	Flat Panel Detector	--
I.I.	Image Intensifier	--
IR	Interventional Radiology	--
PERP	Patient Entrance Reference Point	--
KAP	Kerma Air Product	$Gy\text{-}cm^2$
$K_{a,r}$	Reference Point Air Kerma	Gray (Gy)
$K_{a,r}(d)$	Digital Acquisition Reference Point Air Kerma	Gray (Gy)
$K_{a,r}(f)$	Fluoroscopic Reference Air Kerma	Gray (Gy)
K_{table}	Air Kerma at surface of table	Gray (Gy)
kVp	Kilovoltage Peak	--
mA	Milliamps	--
p	Imager Pixel Size	Millimeters (mm)
PRDMT	Patient Radiation Dose Monitoring and Tracking Systems	--
PSD	Peak Skin Dose	Gray (Gy)
RDSR	Radiation Dose Structured Report	--
SID	Source-to-Image Distance	Centimeters (cm)
SPD	Source-to-Patient Distance	Centimeters (cm)
t	Table Attenuation Coefficient	--

Abstract

Comparison of Peak Skin Dose Calculated by Patient Radiation Dose Monitoring and Tracking Systems versus Solid-State Detector Measurements

By

Vincent Gargaro, B.S.

A thesis submitted in partial fulfillment of the requirements for the degree of Master of Science in Medical Physics

Virginia Commonwealth University

Spring 2022

This study aims to compare the Peak Skin Dose (PSD) that patients obtain from fluoroscopy procedures. The study will show the differences between the PSD measured and calculated from a solid-state detector and the values the unit is displaying. Also, the study will compare PSD measurements from Patient Radiation Dose Monitoring and Tracking Systems (PRDMT). Numerous parameters need to be obtained to depict the PSD that a patient is receiving accurately. The PSD is crucial in assessing the potential biological effects of radiation.

The formalization used to derive the calculated PSD in this study has been established by Jones, A. K., & Pasciak, A. S. et al. All values were obtained through solid-state detector measurements. Measurements were acquired from various radiation generating equipment manufacturers and numerous Patient Radiation Dose Monitoring and Tracking Systems (PRDMT). The PRDMTs that data was obtained from were Imalogix, PEMNET, Radiometrics, and Dosewise. Parameters collected throughout the study were kept consistent for accurate PSD calculations.

Overall, of the units collected, the average PSD obtained from solid-state detector measurements was 1,175 milligray (mGy). Also, the calculated mean PSD from the displayed Air Kerma Rates (AKR) was 1,428 mGy. The results indicate an average 39.4 percent difference between the measured PSD and the PRDMT. Finally, results displayed a 23.1 percent difference between the displayed Air Kerma Rates (AKR) PSD versus the PRDMT.

Introduction

Interventional Radiology (IR) has been used for years in many different medical physics applications. In the late 1890s, the first fluoroscopy unit was developed. At its inception, Willhelm Röntgen was the first to use fluoroscopy procedures truly. He would use a barium platinocyanide screen fluorescing when exposed to “x-rays”. This type of crude viewing was not widely used as it required a radiologist to sit in front of the fluorescent image for periods to observe the procedure. The procedure exposed everyone involved to high amounts of radiation. As the x-ray tube has become readily available, fluoroscopy became more well known. Even though x-ray tubes have changed over the years, the basic principle has remained the same. Within an x-ray tube, an electrical current is applied to a cathode. Electrons will be boiled off from the cathode, which is negatively charged. Once the electrons start to boil off, they are then accelerated inside the housing vacuum towards the anode, which is positively charged. At the anode, they will collide with a target material. The tube potential between the cathode and anode describes the energy of which the x-ray beam will be produced. The higher the potential, the higher the energy. The anode in modern x-ray tubes usually consists of a rotating anode made of tungsten. The contemporary x-ray tube goes under extreme heat, and the rotating anode, along with other mechanisms, causes that heat to be dispersed. The anode is usually made of tungsten, which has an extremely high melting point of 6,191 degrees Fahrenheit or 3,422 degrees Celsius. This phenomenon with the nucleus of the atom of the target material then produces the x-rays needed to image the patient. The

interactions for x-rays to be produced are characteristic and bremsstrahlung radiation. To produce characteristic x-rays, a high-energy electron must collide with an inner shell electron. When the high-energy electron collides, the inner shell electron ejects. This process then leaves a hole within the inner layer of the atom. A cascade process occurs to fill the inner shell, emitting an x-ray photon. Bremsstrahlung radiation, or breaking radiation, is produced by a sudden slowing or deflection of charged particles passing by the nucleus due to the attraction.

After the dangers of fluoroscopy were discovered, there was quite a bit of time until the next significant advancement was made: the use of analog fluoroscopy. Analog employs an image intensifier-video camera system. This type of unit required an x-ray image intensifier—the image intensifier, combined with closed-circuit television systems, made for brighter images. Without the I.I. system, it would no longer be considered analog fluoroscopy. For the period, image intensifiers were state of the art. An I.I. is considered an electronic vacuum and consists of five parts. These is the input phosphor, photocathode, electrostatic focusing lens, accelerating anode, and output phosphor. The Cesium iodide within the housing absorbs the x-rays, emitting light. The photocathode responds to light stimulus, which then emits electrons. The majority of electrons then travel towards the output phosphor via the accelerating electrode. This then produces the image from the procedure.

The next generation of fluoroscopy would come with the advancement of digital electronics. These brought on the use of flat-panel detectors. Flat-panel detectors can work one of two ways: they can convert x-rays into an electrical

charge, which is called direct conversion, or by light, which is called an indirect conversion. Direct detectors generate electron-hole pairs through an internal photoelectric effect. The electrons and holes are drawn to corresponding electrodes by applying a bias voltage to a certain depth within the selenium. The current produced is proportional to irradiation intensity. Indirect detectors contain a photodiode, which generates an electrical signal from light photons. This then produces electron-hole pairs. This requires the FPD to have a thin film transistor that produces a signal that needs to be read out in a specific sequence. Direct detectors are usually made of amorphous selenium or other photoconductor material.[4] The indirect FPDs are typically constructed of a layer of scintillator material such as cesium iodide or gadolinium oxysulfide. There will be an amorphous silicon detector array behind the scintillator layer. Both forms of conversion do need to include the use of thin-film transistors. These transistors contain pixels to form a grid that will be used to capture the x-rays. Even though flat panel detectors cost more, the advantages outweigh the price. The absorption efficiency is much better with the FPDs than with image intensifiers. The earlier I.I. needed to contain a vacuum to get the incoming x-rays for the anode to be readout. The use of FPDs means that the cover can just be made of a thin layer of carbon fiber. There is no longer a need for a closed-circuit television system with FPDs. The smaller housing unit is more useful as the available gantry angles are maximized. Since the image quality improves immensely with digital detectors, it may also reduce the radiation dose to the patient. FPDs enhance the quality of the image by reducing different artifacts from fluoroscopy. These artifacts include

geometric distortion and veiling glare. Also, the detective quantum efficiency (DQE) is much higher with FPDs, resulting in a lower dose to the patient. The DQE measures the combined effects of an imaging system's signal and noise performance.[11] There is always a risk versus reward benefit that is needed to be maximized when looking at the dose to a patient during the procedure. One needs to evaluate the patient's dose and observe if the anatomy being imaged is clear for the procedure.

There is a very distinct difference between stationary radiography units and fluoroscopy. While stationary radiography units are handy for observing broken bones or detecting pneumonia within a patient, fluoroscopy has enormous advantages. Fluoroscopy is advantageous for specific procedures because it is a dynamic x-ray, while radiography is a static image of the patient. This means that the directing physician can see inside of the patient while they are completing a procedure. This allows the physician to visualize the contrast agent is traveling or direct needles for pain management. In one sense, radiography has a lower risk of radiation-induced biological effects because there is less radiation encountering the patient.

Fluoroscopy has progressed even more in recent years. In the 1940s and 1950s, fluoroscopy created the ability to fit people into different size shoes. In the 1970s, the use of a cesium iodide input phosphor was established. This phosphor improved the absorption of the x-ray photons, which was used in conjunction with rare earth intensifying screens. The cesium iodide led to a decrease in patient dose but increased spatial resolution. The use of different contrast agents started to

become prevalent during the 1970s. The contrast agents gave the performing physicians a look inside a patient's blood vessels to observe where the contrast was traveling. In the 1980s, most manufacturers were concerned with more modern imaging equipment such as Computed Tomography (CT) and Magnetic Resonance Imaging (MRI). Even though this is true, the use of digital fluoroscopy started to become more prevalent. There were significant improvements in computer storage, data retrieval, and viewing and recording of patient anatomy. The new fluoroscopy equipment used an imaging plate coated with a europium-activated barium fluorhalide phosphor. The x-ray tube was on one side of the patient, and the x-ray photons passed through the patient reaching the plate, leaving a latent image of the patient's anatomy on the plate. The plate is then scanned, retrieving the image. Since the 1990s, the use of FPDs has become more prominent. Digital Imaging and Communications in Medicine (DICOM) is the standard for the communication and management of medical imaging information. The DICOM header has parameters of each image that is received. This information consists of which location the image was taken, which unit the procedure was performed on, the parameters of the study, patient name, age, and sex. Within DICOM information, each modality has a Radiation Dose Structured Report (RDSR) data which then explains the parameters of the radiation event that occurred. The RDSR data includes all parameters that are needed for the completion of the PSD calculation. Many aspects of fluoroscopy have made the procedures easier for everyone involved. The increase in capabilities has led to better image quality, which has led to the patient being on the table for less time.

This also means that the patient is exposed to less radiation. Better image quality has led to the better treatment of the patient; however, it comes at a high cost.

There is not sufficient information on the dose monitoring of patients during fluoroscopy systems. There are regulatory bodies that do enforce rules and regulations regarding patient monitoring. The Joint Commission states that if a hospital or outpatient clinic provides fluoroscopy services, they must report the cumulative Air Kerma or the Kerma Air Product (KAP). If the system cannot report either of those two, the time of the procedure and the number of images collected must be reported. Also, if a dose threshold for skin is reached, the performing physician must report it to the patient and identify if any further observation is needed. The old definition of a sentinel event is a procedure where a patient receives more than 15 Gray (Gy) to one single field within a 6–12-month period. The new sentinel event is established by the Joint Commission and is stated as a patient safety event that reaches a patient and results in death, severe harm, or permanent harm.[22] The Food and Drug Administration (FDA) also states that after May 19th, 1995, the tube potential and current cannot produce an Air Kerma Rate of higher than 88 milli-gray (mGy) per minute.[20] This dose limit comes from document 10CFR20 presented by the United States Nuclear Regulatory Commission. These regulatory bodies enable the safety of the patient through dose monitoring programs. There are different manufacturers of Patient Radiation Dose Monitoring and Tracking Systems (PRDMT) currently on the market. The study should observe which PRDMT is the best compared to solid-state detector measurements. Some Patient Radiation Dose Monitoring and

Tracking Systems, such as PEMNET, only show the total dose, not the calculation for PSD. Other monitoring systems, such as DoseWise, use data such as the table height, field size, source to surface distance, and source to receptor distance to calculate the PSD. The data is obtained from the unit itself, then displayed within the Radiation Dose Structured Report (RDSR). As stated earlier, RDSR was established to give the reporting physicians a better understanding of how radiation affects patients. The FDA and Joint Commission have set regulations and thresholds to put a standard across the board for facilities that operate fluoroscopy. The monitoring systems that calculate the PSD use corrections for the table's location and the positioning of the x-ray tube and detector. These monitoring systems also take table and pad attenuation correction factors into account. Other factors such as the backscatter and the dose in tissue to air correction factors are imperative for accurate PSD calculations. Also, when calculating the PSD, the gantry angles come into effect to show where the x-ray field is projected onto the patient. Also, the angulation of the gantry plays a significant role on the surface of the patient being exposed. This angulation shows the projected x-ray field onto the patient.

The study compares the unit's Air Kerma Rate versus a solid-state detector measured Air Kerma Rate. The rate displayed from the unit is directly used in calculating the PSD from the Patient Radiation Dose Monitoring and Tracking Systems (PRDMT). The total PSD that the PRDMT estimates can be compared to a formalized hand calculation performed. There is also a hand calculation for each AKR that the unit display and it is then compared to the

solid-state detector measurements. The solid-state detector measurements give the accurate dose that the patient would be receiving during their interventional radiology procedure. This is considered the actual dose as solid-state detectors must be calibrated by certified labs every two years. The solid-state detector gives the accurate dose to the patient by observing the current that develops across the p-n junction when a particle of ionizing radiation travels across it. These charges are then displayed as a signal to show the amount of electron volts (eV) displayed, which can then be converted into dose. [8]

The data for the study was collected from four different hospital systems in six different interventional radiology suites. The hospital systems that were included in the study were: Virginia Commonwealth University (VCU) Medical College of Virginia, located in Richmond, Virginia; Louis Stokes Cleveland Veterans Affairs (VA) Medical Center, located in Cleveland, Ohio; University of Pittsburgh Medical Center (UPMC) Hamot located in Erie, Pennsylvania, and St. Clair Health located in Pittsburgh, Pennsylvania. From these locations, one unit was collected at VCU, two at the VA, one at UPMC Hamot, and two at St. Clair Health.

Methods

The setup during the study is crucial for an accurate calculation of the PSD. The solid-state detector that was used in the study was a Radcal AGMS-DM+. This type of solid-state detector measures many different parameters during exposure. The Radcal AGMS-DM+ measures the kilovoltage peak, or kVp, and the half value layer, or HVL, by two separate detectors within the detector housing. When ionizing radiation encounters the solid-state, a ratio of dose between the two detectors calculates the signal between the two, therefore displaying the kVp. One detector has added filtration and calculates the HVL. The kVp is the tube potential applied to the x-ray tube between the cathode and anode to obtain the needed image for the procedure. The next parameter is the tube current, measured in milliamperes, or mA, and is also used to obtain the best image possible during the examination. The HVL is the thickness of Aluminum added to the beam to make the beam harder. Beam hardening is when a substance is added to the beam to remove the lower energy x-rays from the beam. This lowers the dose to the patient as only the higher energy x-rays are left. These pass through the patient and end up at the detector. The Radcal AGMS-DM+ also measures the amount of time the beam is on, as the study required 20 minutes of procedure time. It should be known that as the HVL increases, the accuracy of a solid-state detector measurement decreases by roughly 5%.[13] It should be noted that moving from 6 to 14 inches of PMMA, the HVL increased from 7.3 to 8.3 millimeters of Aluminum on average. When obtaining the Dose Area Product displayed by the unit, it is measured in units of Gy-cm^2. Therefore, the values

multiplied to obtain the DAP reading are multiplied by the Air Kerma Rate (mGy) and the square area (cm^2) of the activated area of the flat-panel detector built within the unit.

For the data collection portion of the study, everything was kept as consistent as possible from site to site. Dr. Frank Corwin and I did the initial data collection at the VCU Medical Center in Richmond, Virginia. This collection was completed on a Siemens Artis Zee with Pure angiography unit. The source-to-image distance was set to 120 centimeters (cm) for this unit. The source-to-image distance of 120 centimeters is the maximum SID for every tested unit. This was the furthest distance that was capable of this unit. This unit's image intensifier size (I.I.) was set to 32 centimeters.[19] The Veterans Affairs Hospital Systems displayed the I.I. size in inches; therefore, after converting, Room 1 had an I.I. size of 30.48 cm, while Room 2 was 33.02 cm. UPMC Hamot, and St. Clair Room 1 and 2 were consistent with VCU and were 32 cm. The frames per second (FPS) were set to 15. This means that 15 different images were collected and displayed in one second. The Veterans Affairs Hospital Systems Room 1 and UPMC Hamot were consistent with VCU using 15 FPS. The Veterans Affairs Hospital Systems Room 2 used 12 FPS, while both rooms at St. Clair used 7.5 FPS. After consulting with Dr. Frank Corwin, it was determined that the difference in frames per second would not impact the study. Using a certain number of frames per second instead of continuous fluoroscopy usually lowers the patient's dose during the procedure. The unit was also set to be tested in normal mode. There are six main types of fluoroscopy modes used: continuous,

high dose, pulsed, frame averaging, last frame hold, and digital subtracted angiography (DSA). The pulsed acquisition means that a certain number of images are acquired within a certain period. Continuous fluoroscopy is the most basic form of fluoroscopy, which means that the x-ray beam is always on until the user releases the pedal. A high dose rate is used for procedures that allow users to increase the dose rate to 20 Roentgen per minute. This type of fluoroscopy would be used in situations when a physician is imaging a thicker patient or when greater anatomical detail is needed. Frame averaging lowers the patient's dose, takes a series of images acquired, and averages the images together to get the final product. Last frame hold acquisitions are used when the user needs to observe the image without exposing the patient to more radiation with continuous fluoroscopy. The last frame hold keeps the previous image acquired on the display monitor for the physician to observe the anatomy required. Finally, digital subtraction angiography, or DSA, is explicitly used for visualizing blood vessels within a patient. Radiopaque structures, such as bones and high-density material, are subsequently subtracted from the image, therefore leaving only the blood vessels behind.

For the collection, many factors came into account. For the unit at VCU, the first variable that was collected was the distance from the focal spot on the x-ray tube housing to the solid-state detector. This distance is crucial in calculating the PSD as it is needed to complete the inverse square law correction for the distance back to the Patient Entrance Reference Point. The following variable was the Air Kerma Rate (AKR) shown on the unit's display monitor. In conjunction

with the AKR, the tube potential (kVp) and tube current (mA) that the unit displayed was also collected. The unit's kVp depends entirely on the amount of material (patient's thickness) within the beam when the unit is producing radiation. The Automatic Dose Rate Control (ADRC) is put into place to keep the signal-to-noise ratio of the image constant. It completes this by regulating the x-ray exposure rate incident on the I.I. or FPD. When the system is panned from a region of low attenuation to one of greater attention, fewer x-rays strike the detector. Once this occurs, the ADRC sends a signal to the x-ray generator to increase the rate of x-ray exposure.

The Seissl Method, named after Siemens engineer Johann Seissl, is a method where the spectral filter varies the added filtration needed according to the thickness of PMMA used in the study within Task Group Report 125.[15] When increasing the thickness of PMMA, the thickness of the filter decreases due to the patient attenuating more of the beam. The spectral filter thickness was placed in the beam by the machine during the study. This filter then makes the beam harder, which removes the low-energy x-rays. By this logic, less dose is delivered to the patient as the higher energy x-rays pass through the patient. These high-energy x-rays then make it to the detector to correctly display the image needed for the procedure at hand. The filter for interventional radiology use is usually made of copper. The other filtration metals that are used occasionally are Aluminum and tantalum. The higher the kVp, the thinner the amount of copper needed. This is due to the patient being thicker and consequently hardening the beam.

Figure 1: Shows the setup of the study with 6 inches of PMMA on top of the cutout in the correction location over the x-ray tube with the patient table removed.

Figure 2: Shows the setup of the study with 14 inches of PMMA on top of the cutout in the correction location over the x-ray tube with the patient table removed.

As one can see from Figures 1 and 2 above, this is the setup used for the data collection portion of the study. The specially designed table has a cut-out in the middle that allows for negligible attenuation to the solid-state detector. In this picture, the x-ray source is below the table. Then, the attenuation material that acts as the patient, or PMMA, are the square pieces on top of the table. The first run completed simulated six inches of a patient with six inches of PMMA equivalent for the study. The patient thickness was then increased to 14 inches of

PMMA to simulate a thicker patient. Underneath the slabs of PMMA is the solid-state detector (not pictured) that was used to measure the amount of radiation detected. As mentioned before, the table with the cut-out in the center is next. This cutout allows the solid-state detector to sit underneath the PMMA without attenuating material underneath. This table then sits below the I.I. The I.I. is used to collect all the photons produced, which then displays the image of what the photons just passed through. Below are two schematics are taken from Task Group Report 272 that are explained above.[12]

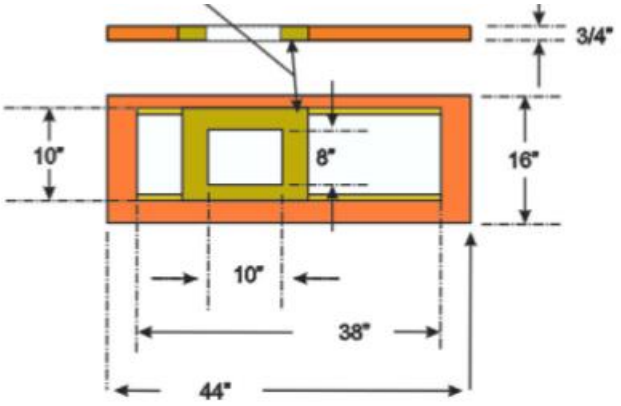

Figure 3: TG 272 specially designed table used in study[12]

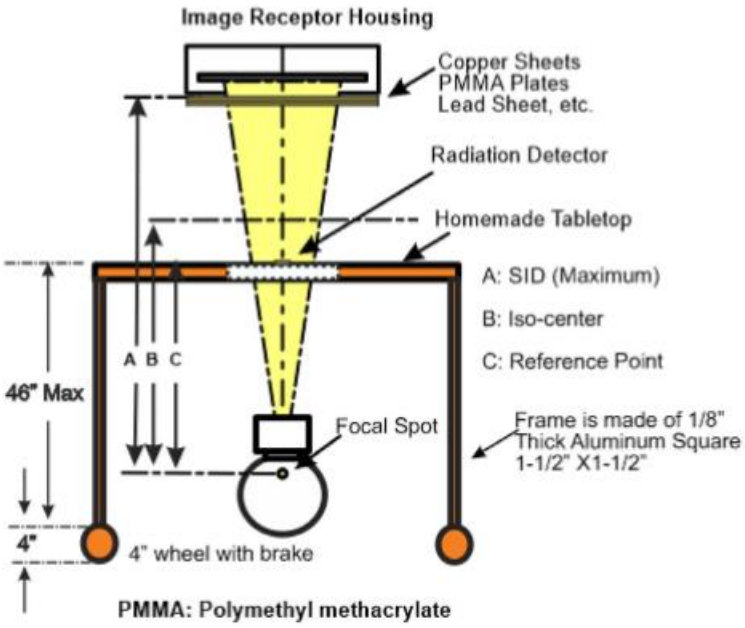

Figure 4: TG 272 specially designed table used in study[12]

Many different factors come into play when looking at the PSD that a patient receives during an IR exam. These factors combined will give us the result of the PSD. Peak skin dose needs to be closely monitored, as there are possible different biological effects. Even though the purpose of this study was not to detail what these effects are, it is essential to mention that they are there, and therefore the PSD needs to be monitored for each patient.

The following procedure of the study was to consider which calculation would be used to complete the hand calculation from the data retrieved off the machine with the solid-state detector. When comparing different methods, such as

Task Group Report 190, for this calculation, one seemed the most adequate for this study. This is the calculation formulized by Jones, A. K., & Pasciak, A. S.

The first calculated step was the projected x-ray field on the patient from the IR unit for this calculation. The projected x-ray field size is the square field projected on the patient from the collimated field. The symbol of A_{skin} gives this formula. The formula for the projected x-ray field size is given:

$$A_{skin} = \left[\left(\left|C_{Left} - C_{Right}\right| * \left(\frac{p}{10}\right)\right) * \left(\left|C_{Upper} - C_{Lower}\right| * \left(\frac{p}{10}\right)\right)\right] * \left(\frac{SPD}{SID}\right)$$

Equation 1: Showing equation for projected x-ray field on patient.[10]

As shown in the above equation, moving from left to right, the C_x variable refers to the collimator position. The collimator position has units of pixels. The number of pixels can be obtained from the units manufacturer brochure. The variable of p is labeled as the imager pixel size. The imager pixel size can also be obtained from the manufacturer's brochure but has units of millimeters (mm). This allows one to collimate with the square collimator setting manually. For the simplicity of the study, the collimator was set to a square. It should be known that the Image Intensifier size is the diagonal of the square. Meaning, that if one were to use a 32-centimeter I.I., the diagonal of the projected I.I. would be 32 centimeters. Continuing, the variable of SPD is the Source-to-Patient distance. This distance is from the x-ray tube to the surface of the patient, and is measured in centimeters. The Source-to-Image distance, or SID, is the distance from the x-

ray source to the Image Intensifier. This distance, measured in centimeters, was constant for all units to keep consistency between hospital systems.

The following equation is needed to complete the Digital Acquisition point Air Kerma calculation. This is the total Air Kerma that is perceived to be accumulated by the patient. The units for this Air Kerma are given by Gray (Gy) and the formula of:

$$K_{a,r}(d) = \frac{KAP}{A_{skin}}$$

Equation 2: Showing calculation for Total Air Kerma.[10]

The KAP, or Kerma Air Product, is calculated by taking the produced Air Kerma multiplied by the x-ray field size. The units of KAP are Gray centimeter squared or Gy-cm^2. The KAP is then divided by the projected x-ray field size on the patient to obtain the Total Air Kerma Produced.

Once the Total Air Kerma that the patient received was obtained, Equation 2 was completed. The next step was to complete the Reference Point Air Kerma calculation at the table surface. The variable for this is $K_{a,table,}$ and has units of Gray (Gy). It should be known that the table height and the detector distance from the focal spot of the x-ray tube are not at the PERP. The formalization for the Air Kerma at the table surface is given by:

$$K_{a,table} = K_{a,r} * (\frac{d_{source} - to - PERP}{d_{source} - to - patient})^2$$

Equation 3: Calculation for the Air Kerma at the surface of the table.[10]

From this calculation, we can see that this considers three significant factors.

First, the total Air Kerma was calculated in Equation 2, and two other distance correction factors were obtained. The first is in the numerator of the equation, being the d_{source}-to-PERP. This factor is known as the variable of the distance from the x-ray producing source to the PERP, or Patient Entrance Reference Point. The PERP is the distance from the x-ray source to the isocenter, then fifteen centimeters back towards the x-ray source. The isocenter is a point in space on the beam's straight axis. The isocenter can be found by finding the focal spot on the housing of the x-ray tube and measuring the specific distance specified by the manufacturer. The PERP is crucial in this calculation as this is the point to which every manufacturer calculates the dose from the unit. The denominator of this equation is the distance from the x-ray source to the entrance of the patient's skin. This is given by the variable of d_{source}-to-patient. For the study, the d_{source}-to-patient distance is the path from the x-ray source focal spot to the surface of the detector. It should be noted that both distances have units of centimeters (cm). This corrects for the difference in distance of the PERP to where you are measuring the radiation. This should show the true dose that the patient is receiving from the procedure. This is known as the inverse square law.

Once these three variables were established, the Entrance Skin Air Kerma calculation was completed. This formula considers the Air Kerma at the table surface and the attenuation of the table. The attenuation of the clinically used table is significant in this calculation because once an x-ray beam is attenuated any amount, the lower energy x-rays are being stopped therefore making the average Kilovoltage Peak, or kVP, higher. When the average kVp of an x-ray beam is higher, technically, the dose to the patient is lower due to more x-rays passing through the patient and reaching the Image Intensifier. The formula for the Entrance Skin Air Kerma is formalized as:

$$ESAK = K_{a,table} \times t$$

Equation 4: Calculation of Entrance Skin Air Kerma (ESAK).[10]

As illustrated from Equation 4, the ESAK takes the Air Kerma at the table surface multiplied by t, which is the table attenuation coefficient. The table attenuation coefficient is a constant for every table height and tube angulation. The attenuation coefficient varies on the kVp used but is tabulated and published information. The table attenuation coefficient does not have any units, making the units of the ESAK to be Gray (Gy). Below are the tabulated table attenuation coefficients are taken from Task Group Report 272.[12]

		Tube potential (kVp)							
		60	70	80	90	100	110	120	Average
SSF (mmCu)	0	0.587	0.611	0.628	0.64	0.653	0.661	0.669	0.635
	0.1	0.635	0.659	0.675	0.683	0.691	0.699	0.704	0.678
	0.2	0.651	0.676	0.687	0.697	0.704	0.711	0.715	0.691
	0.3	0.657	0.684	0.697	0.707	0.713	0.719	0.722	0.7
	0.6	0.679	0.701	0.711	0.718	0.723	0.729	0.732	0.713
	0.9	0.692	0.708	0.726	0.723	0.729	0.733	0.736	0.721
	Average	0.65	0.673	0.688	0.695	0.702	0.709	0.713	

Table 1: Table attenuation factors varying with tube voltage[12]

Even though the next equation is a constant and is published information, there needs to be an explanation of what the variable means and how it is calculated for the study. The next variable is the f-factor. It has the units of Gray per Roentgen or Gy/R. It is given by the equation:

$$f_{medium} = \frac{(\frac{\mu_{en}}{p})_{medium}}{(\frac{\mu_{en}}{p})_{air}}$$

Equation 5: The ratio of absorption rates to a medium.[10]

From Equation 5, both variables in this formula are related to absorption coefficients. The f-factor converts the Air Kerma to dose in a medium. The medium in my study was soft tissue.

Once we have all the variables from Equations 1 through 5, it is time to put them all together to complete the total calculation of the Peak Skin Dose (PSD). The PSD has the units of Gy and is given by the formula:

$$PSD = ESAK * BSF(HVL) * f_{tissue}(kVp)$$

Equation 6: Calculation for Peak Skin Dose (PSD) to patient.[10]

From Equation 6, the PSD is calculated by taking the ESAK from Equation 4 multiplied by a Back Scatter Factor. The BSF considers any amount of radiation that could have backscattered towards the x-ray source and was not detected by the detector. The BSF is published in many different scholarly journals and is a constant across all for the medium of soft tissue. This is then multiplied by the f-factor from Equation 5, a constant. Multiplying all three of these variables will give you a rough estimate of a PSD calculation. Below are two tables that show BSF according to kVp.[16] For simplicity within the study, the BSF was consistent throughout all calculations at 1.4.

Tube voltage (kV)	Filter	Backscatter factor (B)									
		Field size	100 mm × 100 mm			200 mm × 200 mm			250 mm × 250 mm		
		HVL (mm Al)	Water	ICRU tissue	PMMA	Water	ICRU tissue	PMMA	Water	ICRU tissue	PMMA
50	2.5 mm Al	1.74	1.24	1.25	1.33	1.26	1.27	1.36	1.26	1.28	1.36
60	2.5 mm Al	2.08	1.28	1.28	1.36	1.31	1.32	1.41	1.31	1.32	1.42
70	2.5 mm Al	2.41	1.30	1.31	1.39	1.34	1.36	1.45	1.35	1.36	1.46
70	3.0 mm Al	2.64	1.32	1.32	1.40	1.36	1.37	1.47	1.36	1.38	1.48
70	3.0 mm Al +0.1 mm Cu	3.96	1.38	1.39	1.48	1.45	1.47	1.58	1.46	1.47	1.59
80	2.5 mm Al	2.78	1.32	1.33	1.41	1.37	1.39	1.48	1.38	1.39	1.50
80	3.0 mm Al	3.04	1.34	1.34	1.42	1.39	1.40	1.51	1.40	1.41	1.52
80	3.0 mm Al +0.1 mm Cu	4.55	1.40	1.40	1.49	1.48	1.50	1.61	1.49	1.51	1.63
90	2.5 mm Al	3.17	1.34	1.34	1.43	1.40	1.41	1.51	1.41	1.42	1.53
90	3.0 mm Al	3.45	1.35	1.36	1.44	1.42	1.43	1.53	1.42	1.44	1.55
90	3.0 mm Al +0.1 mm Cu	5.12	1.41	1.41	1.50	1.50	1.51	1.62	1.51	1.53	1.65
100	2.5 mm Al	3.24	1.34	1.34	1.42	1.40	1.41	1.51	1.41	1.42	1.53
100	3.0 mm Al	3.88	1.36	1.37	1.45	1.44	1.45	1.55	1.45	1.46	1.57

Table 2: Back-scatter factors varying with tube voltage[16]

Tube voltage (kV)	Filter	Backscatter factor (B)									
		Field size	100 mm × 100 mm			200 mm × 200 mm			250 mm × 250 mm		
		HVL (mm Al)	Water	ICRU tissue	PMMA	Water	ICRU tissue	PMMA	Water	ICRU tissue	PMMA
100	3.0 mm Al +0.1 mm Cu	5.65	1.41	1.42	1.50	1.51	1.53	1.64	1.53	1.55	1.66
110	2.5 mm Al	3.59	1.35	1.35	1.43	1.42	1.43	1.53	1.43	1.44	1.55
120	3.0 mm Al	4.73	1.37	1.38	1.46	1.46	1.48	1.58	1.48	1.49	1.60
120	3.0 mm Al +0.1 mm Cu	6.62	1.41	1.42	1.50	1.53	1.54	1.64	1.54	1.56	1.67
130	2.5 mm Al	4.32	1.36	1.36	1.44	1.44	1.45	1.55	1.45	1.47	1.57
150	2.5 mm Al	4.79	1.36	1.36	1.44	1.45	1.46	1.55	1.46	1.48	1.58
150	3.0 mm Al	6.80	1.39	1.39	1.47	1.50	1.51	1.61	1.52	1.53	1.63
150	3.0 mm Al +0.1 mm Cu	8.50	1.40	1.41	1.48	1.53	1.54	1.64	1.55	1.57	1.67

Table 3: Back-scatter factors varying with tube voltage[16]

Results

When looking at the steps to complete the hand calculation of the PSD from measured Air Kerma, the first was to observe the I.I. size for all the different manufacturers used for this study. When looking at the I.I. size displayed on the display unit, the size shown is the diagonal if the collimated field is a square. The unit used at VCU is a Siemens Artis Zee with Pure Angiography Unit. This unit displayed an I.I. size of 32 centimeters. Per the brochure from Siemens, the Artis Zee with Pure has the largest I.I. size of 48 centimeters with a matrix size of 2,480 by 1,920 pixels.[19] It should be known that the 48-centimeter I.I. size is a rectangle. The largest detector size for the Siemens Artis Zee with Pure is 38 centimeters by 30 centimeters. This means that for a magnification size of 32 centimeters, the detector would be 22 centimeters by 22 centimeters. By simple calculation of a right triangle, the detector size is now 1,421 by 1,421 pixels with the 32-centimeter diagonal I.I. size. Also, from the Siemens brochure, the imager pixel size (p) is known to be 154 micrometers (μm) (Image Technology News). As mentioned in the methods chapter of this paper, the SID for this study was constant across all studies and is known to be 120 centimeters. The SPD was different for each study as the x-ray source varied because the tube under the table was at different heights off the ground. The table that held the solid-state detector and PMMA has a fixed height. Therefore, the only variation between hospital systems could be the location of the x-ray source. The SPD used for VCU was measured at 70 centimeters. With all these variables, we can now complete Equation-1. It is given by:

$$A_{skin} = \left[(1421.5 + 1421.5) * \left(\frac{.0154}{10}\right) * (1421.5 + 1421.5) * \left(\frac{.0154}{10}\right)\right] * \left(\frac{70}{120}\right)$$

This calculation showed a square projected x-ray field size of 11.7 centimeters squared (cm^2) for the Artis Zee with Pure Angiography unit.

Even though this calculation stays constant for all the studies, some parameters may change because different manufacturers use different numbers for their units. For the Toshiba Infinix located at the Veterans Affairs Hospital, the matrix size was 1,320 by 1,320 pixels.[8] Also, the imager pixel size was 194 micrometers (μm). For the Toshiba Infinix, the I.I. size was listed in inches instead of centimeters like all the other units. After discussing with my advisor Dr. Frank Corwin, we established that the I.I. size of 12 inches (30.48 cm) best aligned with the other tested units. Finally, the distance for the SPD was measured to be 60 centimeters (cm). Completing the same calculation for VCU, we established that the projected x-ray field on the patient for the Infinix is 13.1 centimeters squared (cm^2). As previously shown, checking each variable within the calculation was completed for the other four units.

The following calculation is completing Equation-2 for the total Air Kerma. The first step in achieving this was finding the Kerma Air Product (KAP) by taking the Air Kerma that was measured multiplied by Equation-1. Equation-2 is simple as it is taking the KAP divided by the projected x-ray field on the patient from Equation-1. The formula then gives:

$$K_{a,r}(d) = \frac{13944\ mGy - cm^2}{11.723\ cm^2}$$

This gives a Total Air Kerma of 1,247 milligray (mGy). This will be different for each unit measured as they all had different Air Kerma Rates and projected x-ray fields depending on the size of the Image Intensifier and the collimated fields. It should be known that if the Total Air Kerma is obtained from either solid-state measurements or displayed from the unit, Equation 1 does not need to be completed. Equation 2 is equal to the Total Air Kerma that is displayed or measured. Completing Equation 1 is appropriate if the Air Kerma is unobtainable.

Using the results from Equation-2, one could then find the Air Kerma at the table's surface. To calculate this, it is needed to find the Patient Entrance Reference Point (PERP) for each manufacturer. This data is publicly available or is usually posted within the RDSR data transmitted from each unit. The distance of the x-ray source to the solid-state detector was the variable of x-ray source to patient distance. Equation 3 shows that the Total Air Kerma is multiplied by the ratio of the distances of the PERP and from the x-ray source to the patient squared. Equation 3 then went as follows:

$$K_{a,table} = (1{,}247.111\ mGy)(\frac{63.5\ cm}{70\ cm})^2$$

This showed that the Air Kerma at the table's surface for the twenty, one-minute procedures with the two different thicknesses of PMMA was 1,026 milligray (mGy). This procedure was then done for each of the other five units calculations. As stated before, the Air Kerma at the surface of the table varied with each

analysis as each manufacturer had different PERP's and the distances of the x-ray source to the surface of the patient changed with each. Firstly, VCU's Siemens Artis Zee with Pure IR unit has a manufacture PERP of 63.5 centimeters (cm). The two units at St. Clair Health were also Siemens units. Therefore, they also had a PERP of 63.5 cm. The GE Innova, installed at UPMC Hamot, has a reported PERP of 57 cm, the lowest out of all units studied. The IR unit in Room 1 of the Veterans Affairs Hospital was a Toshiba Infinix. Toshiba has a reported PERP of 66 cm. Finally, Philips reports that the Alura XPER FD20, which the Veterans Affairs has in Room 2, has a PERP of 66.5 cm.

Once the Air Kerma at the table's surface had been obtained, the Entrance Skin Air Kerma was calculated. This is calculated by taking the results from Equation 3 and multiplying it by the table attenuation factor of t. The table attenuation factor is tabulated and retrieved from the RDSR data presented at the end of the procedure. It remains constant no matter the kVp and mA that are used. Showing this, the formula came to be:

$$ESAK = 1{,}026.258\, mGy * 0.75$$

The table attenuation factor does not have units, making the Total Entrance Skin Air Kerma for the Siemens Artis Zee with Pure Angiography Unit from VCU MCV was 770 milligray (mGy). The table attenuation correction was 0.75 for all units to keep the calculation consistent.

The final step in calculating the PSD is obtaining the BSF and the f-factor for the final calculation. The BSF was obtained from the RDSR data or published

literature and kept constant for all calculations. The f-factor was obtained from either the kVp or Half Value Layer (HVL) from the graphs below:

	f-factor	
kVp	***Fluoroscopic Mode***	***Digital Acquisition Mode***
60	1.061	1.056
65	1.063	1.058
70	1.065	1.059
75	1.066	1.061
85	1.068	1.063
95	1.069	1.066

Table 4: f-factors for Peak Skin Dose calculation using the kilovoltage peak (kVp) used during the procedure.[10]

HVL (mm Al)	***f-factor***
3.0 – 3.5	1.058
3.5 – 4.0	1.059
4.0 – 4.5	1.061
4.5 – 5.0	1.062
5.0 – 5.5	1.062
5.5 – 6.0	1.063
6.0 – 6.5	1.066
6.5 – 7.0	1.068

Table 5: f-factors for Peak Skin Dose calculation using the Half Value Layer (HVL).[10]

The HVL was collected for half of the units and was used in this calculation. The kVp method was used on the other three units. The average HVL for UPMC Hamot was 7.8 millimeters of Aluminum, ranging from 7.3 to 8.3 millimeters

Aluminum. St. Clair Room 1 had an average HVL of 7.08 millimeters of Aluminum, ranging from 5.7 to 8.5 millimeters Aluminum. Finally, room 2 at St. Clair had an average HVL of 6.01 millimeters of Aluminum with a range from 5.4 to 6.7 millimeters of Aluminum. The value was interpolated according to what the displayed kVp was. Once the BSF and the f-factor are obtained, the PSD calculation can be completed as follows:

$$PSD = 769.6933\ mGy * 1.4 * 1.067$$

This gave a Total Measured PSD for the Siemens Artis Zee with Pure from VCU of 1153 milligray (mGy).

$$A_{skin} = \left[(1421.5 + 1421.5) * \left(\frac{.0154}{10}\right) * (1421.5 + 1421.5) * \left(\frac{.0154}{10}\right)\right] * \left(\frac{70}{120}\right)$$

$$K_{a,r}(d) = \frac{13944\ mGy - cm^2}{11.723\ cm^2}$$

$$K_{a,table} = (1{,}247.111\ mGy)\left(\frac{63.5\ cm}{70\ cm}\right)^2$$

$$ESAK = 1{,}026.258\, mGy * 0.75$$

$$PSD = 769.6933\, mGy * 1.4 * 1.067$$

$$PSD = 1153\, mGy$$

The above flow chart shows the PSD for the measured AKRs taken from VCU. The chart below shows all other calculations for comparing the other five units obtained.

	A	B	C	D	E	F	G	H	I
1		A_{skin} (cm^2)	KAP (mGy-cm^2)	$K_{a,r}$ (mGy)	$K_{a,table}$ (mGy)	ESAK (mGy)	BSF	f-factor	PSD
2	**VCU**	11.18	13945	1247	1026	770	1.4	1.064-1.07	1153
3	**VA-Wade Park Room 1**	13.12	12876	982	1188	948	1.4	1.065-1.0685	1418
4	**VA-Wade Park Room 2**	12.43	9937	800	812	623	1.4	1.065-1.07	933
5	**UPMC Hamot**	5.41	6806	1257	1116	857	1.4	1.069-1.071	1285
6	**St. Clair Room 1**	10.97	14643	1335	1255	964	1.4	1.062-1.068	1441
7	**St. Clair Room 2**	11.39	9315	818	713	548	1.4	1.062-1.0685	819

Table 6: Calculated values for all 6 units tested

The Dose Area Product was displayed at the end of each procedure. Below are the six Dose Area Product's displayed from each unit. The Dose Area Product (DAP) has the same units as the Kerma Air Product (KAP) of Gray centimeter squared (Gy-cm^2).

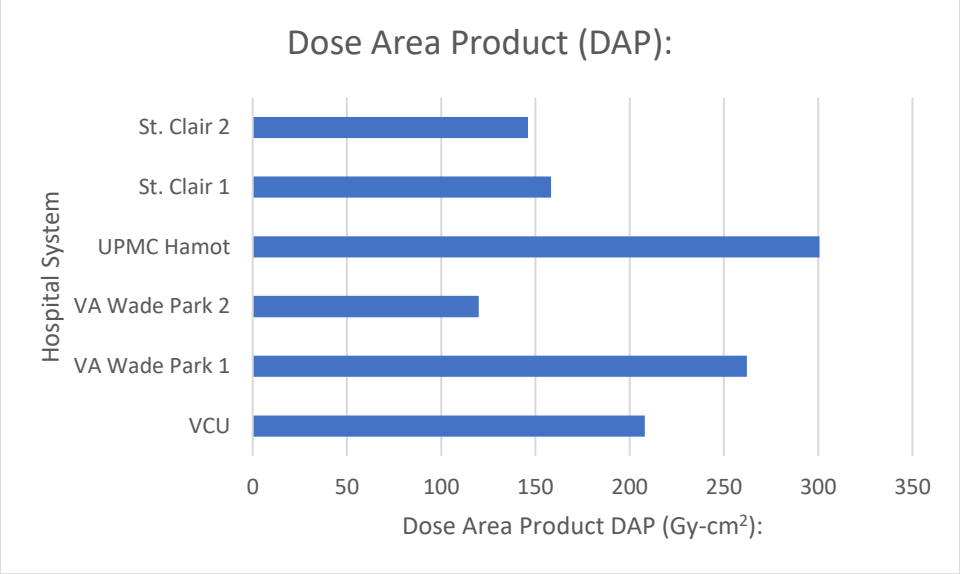

Graph 1: Comparison of the Dose Area Products (DAP) produced by all six units

As one can see, the unit from UPMC Hamot had the highest DAP reading at 300 Gy-cm^2, while the Veterans Affairs Room 2 had the lowest DAP reading at roughly 120 Gy-cm^2.

In addition, all of the calculations were completed for each of the units displayed AKRs. The only factor that was changed for the completion of the calculation of the units displayed PSD was the variation of what the displayed AKR was from the unit. This calculation gives the difference between the true

value of the PSD (measured) versus what the AKR from the unit is displaying the PSD to the patient (displayed).

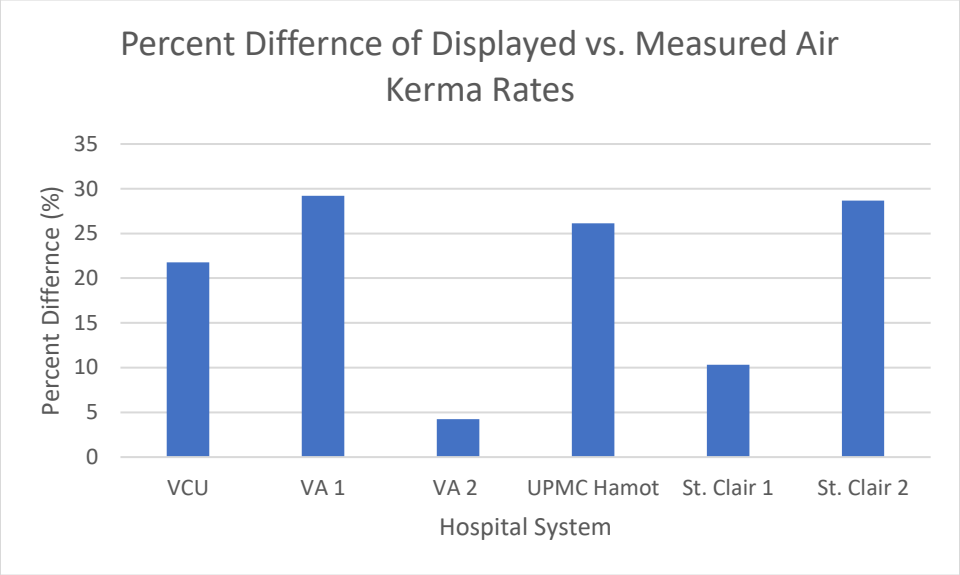

Graph 2: Percent difference of the measured and displayed Air Kerma Rates

As illustrated from the above graph, the percent difference between the measured and displayed Air Kerma's ranged from 4.25% at the Veterans Affairs Hospital on their second unit to 29.22% at the Veterans Affairs on their first unit. This difference between displayed and measured values plays a direct role in calculating the PSD between what the unit and the measured values will end up being. This value and the distances between the measured and the PERP are the only values changed in the calculation. Even though this is true, the PERP does not play a direct role in calculating measured values as the Inverse Square Law correction, which interpolates the Air Kerma then being at the PERP, was performed.

When comparing all the PSD hand calculations, we obtain the graph below.

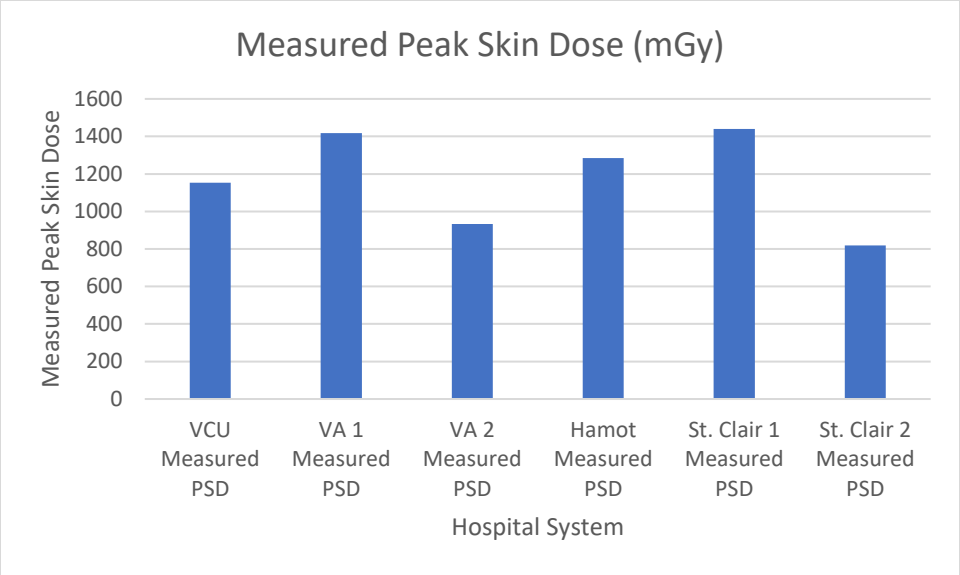

Graph 3: Comparison of the calculated Peak Skin Doses from solid-state detector measurements

The above graph shows that the PSD for St. Clair Room 1 was the highest, while the PSD for St. Clair Room 2 was the lowest. The PSD ranged from 819 mGy to 1,441 mGy, with an average of 1,175 mGy over all six units.

After completing the PSD calculation from the measured Air Kerma Rates, the hand calculation for the units PSD using the Air Kerma Rates displayed during the procedure was obtained. Also, since this value is corrected to the PERP, the Air Kerma at the table's surface and the Total Reference point Air Kerma was known to be the same. In the graph below, one can see the comparison of the unit's PSD totals.

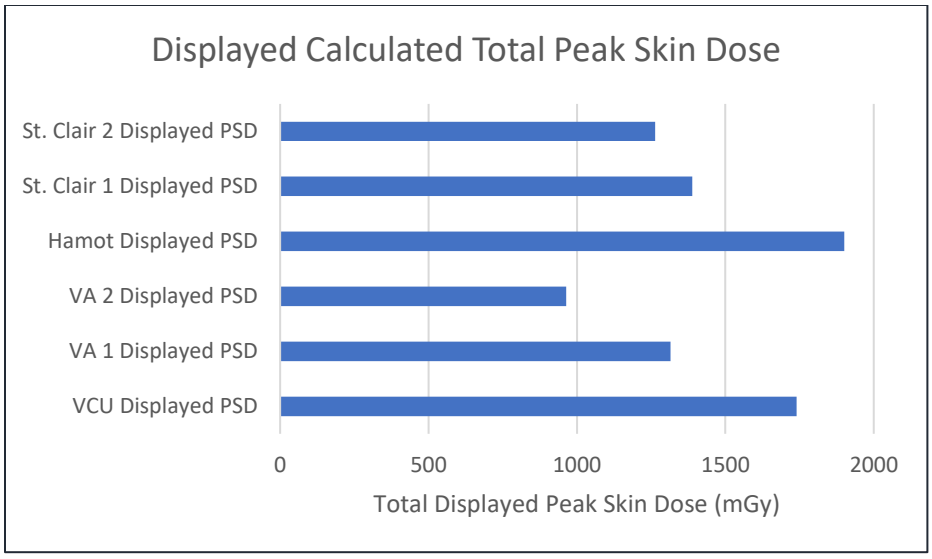

Graph 4: Comparison of Unit Peak Skin Dose calculations for all six units

From the above graph, the PSD of the unit's hand calculation was the highest for UPMC Hamot, with a total PSD of 1,900 mGy. Also, from the graph, the value of 963 mGy shows the lowest value of PSD from Room 2 at the Veterans Affairs Hospital in Cleveland, Ohio. The overall average of all six units was calculated to be 1,428 mGy.

Then, there was the comparison of hand calculations of the unit versus the measured PSD. The comparison of these two sets of values is shown in the graph below.

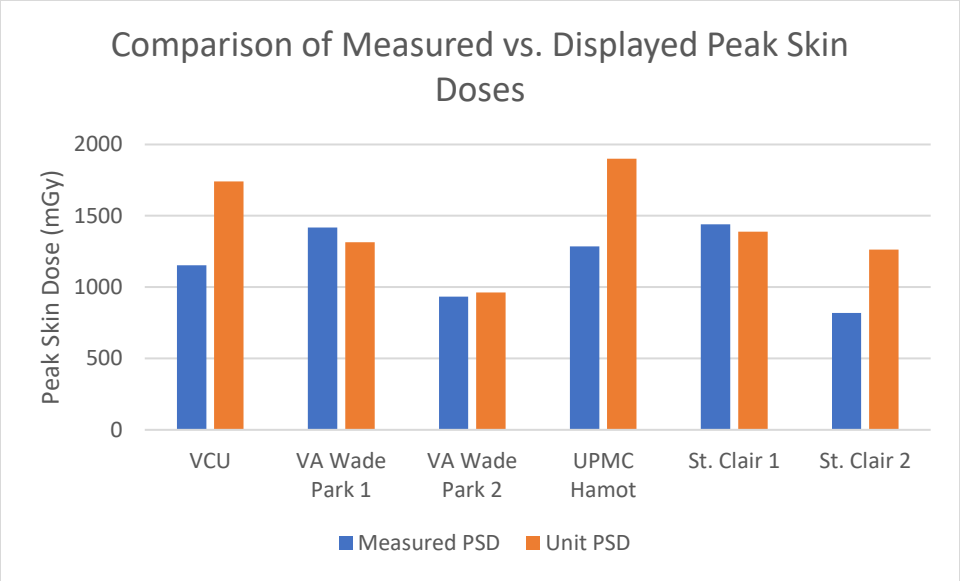

Graph 5: Comparison of Measured Peak Skin Does versus Unit Peak skin dose

This graph shows the percent difference between the hand calculation of the PSD from displayed AKRs and the measured hand calculation of the PSD of VCU, the Veterans Affairs Room 1, the Veterans Affairs Room 2, UPMC Hamot, St. Clair Room 1, and St. Clair Room was 50.9%, -7.23%, 3.22%, 47.88%, -3.64%, and 54.21% respectively. The Veterans Affairs Room 2 had the best comparison between the unit and measured PSD calculations. The PSD at this location was the lowest as well. The difference between the units PSD and the measured PSD was the largest for St. Clair Room 2. This was a difference of 34.48%. This is significantly large, as a dose displayed by the unit of 1,000 mGy means that the true dose would be 655.2 mGy. This comparison shows the true dose (measured values) versus the dose that the patient would be receiving if this hand calculation

was used. The only parameter that was changed was the Air Kerma used for the calculation.

There is a comparison of the hand calculation of the PSD from the AKR the unit displayed versus the PSD from the PRDMT. Theoretically, these two should be the same value as the Air Kerma that the unit displayed, and what is used from the RDSR data in the PRDMT is equivalent. Even though, theoretically, the two values should be the same, the PRDMT uses an algorithm that is unknown to the public that manipulates a variety of factors to calculate the final dose they display. The two PRDMTs used for this study were Imalogix (VCU) and DoseWise (Veterans Affairs). The graph below shows the PSD of the hand calculation from the unit and the PSD displayed from the PRDMT.

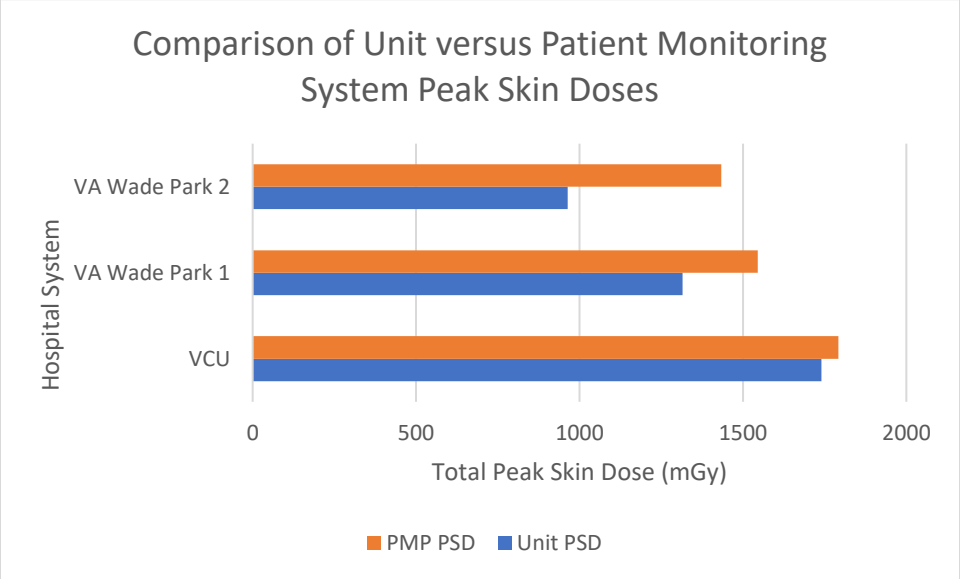

Graph 6: Comparison of Unit Peak Skin Dose versus Peak Skin Dose from the Patient Radiation Dose Monitoring and Tracking Systems

As shown in Graph 6, the PSD from Imalogix at VCU is exceptionally close to the hand calculation of the units displayed Air Kerma Rates PSD calculation. This

came to a difference of 3.01%. The PSD from DoseWise at the Veterans Affairs Hospital in Cleveland, Ohio, had a little larger difference between the calculation of units PSD. This came to 17.46% and 48.81%, respectively, for Room 1 and Room 2 at the VA.

Finally, a comparison of the PSD from the two different PRDMT to the hand calculation from the measured Air Kerma Rates was observed. The graph for this comparison is below.

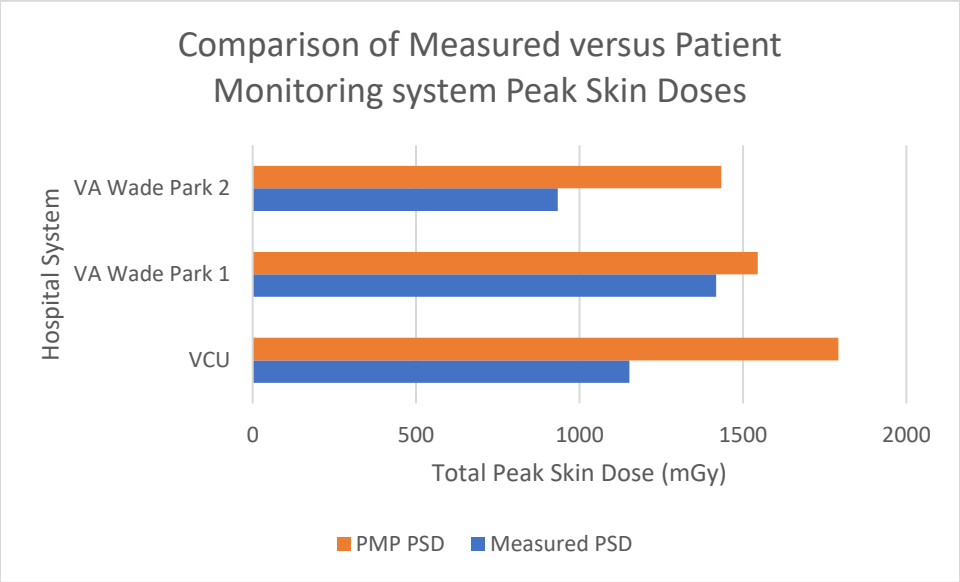

Graph 7: Comparison of Measured Peak Skin Dose versus Peak Skin Dose from the Patient Radiation Dose Monitoring and Tracking Systems

Looking at Graph 7, the lowest PSD difference between the PRDMT and the measured hand calculation comes from DoseWise in Room 1 at the Veterans Affairs. This difference came to 8.97%. The other room at the Veterans Affairs had a difference of 53.60% using DoseWise, while Imalogix had a difference of 55.5% difference at VCU.

Sources of Error

There could be a few possible sources of error that could have occurred during my study. The first source of error is that there is allowed to be a difference of up to 35 percent between the measured and displayed values of the Air Kerma Rates. Since this is a crucial part of the PSD calculation, the calculated value of the measured and the units PSD could vary vastly. The FDA is the organization that has put this rule into effect. It states that the unit had to be manufactured on or after June 10th, 2006.

Along with the variation in the Air Kerma Rates, this could lead to variations between the Dose Area Product (DAP) values compiled by the units. This is due to the uncertainties within the Ionization Chamber that is built within the unit of the fluoroscopy unit. This ionization chamber has an uncertainty of roughly 5%, which is constant for all fluoroscopy units. The solid-state detector also has an uncertainty of approximately 5%. The DAP meter within the unit can be calibrated, and a certified service engineer does this. This is done by measuring the dose over the entire beam at a known distance with a small volume ionization chamber and comparing the results.

Also, there could be some variation of error within the PRDMT itself. The PRDMT and the unit could not be fully synced together, and some source of error could arise. This could be from the table height not being in the exact location the PRDMT believes it is, or the same could happen for tube angulation. These factors would vary the PSD calculation, as seen from the previously discussed

equations. Task Group Report 272, Appendix E gives various measurements to ensure accurate data is being sent to the RDSR for correct PSD calculations.[12]

Along with these error sources, it takes some time for the x-ray source to start and produce radiation when you stand on a fluoroscopy pedal. The below waveform shows that, even though possible, no significant amount of pulses were missed during the data collection.

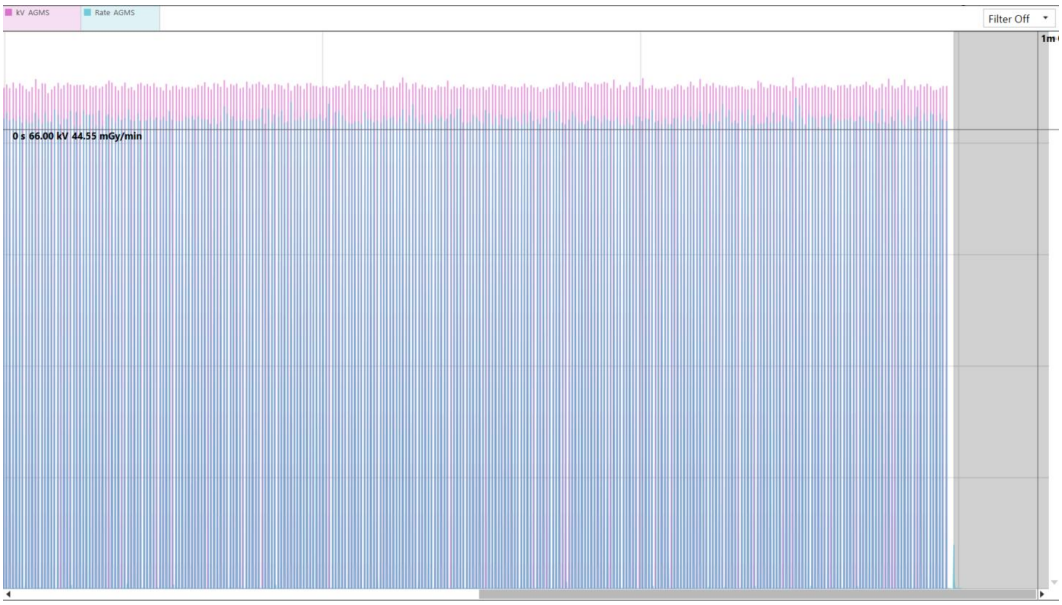

Figure 5: Waveform of the collected pulses from study collected from Radcal AGMS-DM+.

Conclusion

After analysis, evidence shows a difference between the measured and the units calculated PSD values. Even though the variables within the calculation were kept the same, the results show an average of 24.2% difference between the calculation from the measured values to the displayed values. There was a maximum difference of 54.21% between the two values, with a minimum of 3.22%.

When comparing the differences between the displayed PSD and the PRDMT, there was an average of 23.093% between the two values obtained for the calculated and the PRDMT. The PSD had a minimum difference of 3.014% with a maximum difference of 48.1%.

The differences between the measured PSD and the PSD from the PRDMT were more pronounced. The average difference between the two PSD values was 39%. The most significant difference came to be 53.59%. The smallest showed a difference in PSD values of 9%.

This difference could be significant when looking at possible biological effects occurring to a patient. If the measured and displayed Air Kerma Rates are off by more than plus or minus 35 percent, the physicist is responsible for alerting the service engineer that calibration needs to be performed on the machine to correct this action. It is understood that the dose that the PRDMT is reporting should consequently be higher due to a buffer being incorporated into the calculation. If the doses reported are higher, the effects are not happening due to

this buffer zone. Keeping this buffer zone to a minimum is essential because if it is too large, then every patient undergoing a fluoroscopy procedure will have to be evaluated after the procedure to ensure that these effects are not occurring.

References

1. *ACCU-Gold2 User Guide*. PDF Free Download. (n.d.). Retrieved October 6, 2021, from https://docplayer.net/53945059-Accu-gold2-user-guide.html.
2. *Artis zeego - umetex.ru*. (n.d.). Retrieved October 6, 2021, from https://umetex.ru/wa-data/public/shop/manuals/Siemens_Artis_zeego.pdf.
3. *Artis zee with pure tackle every challenge*. (n.d.). Retrieved September 28, 2021, from https://www.deltamedicalsystems.com/wp-content/uploads/2021/02/ARTIS-Zee-Brochure-10-2019.pdf.
4. Ashworth, J. (2019, July 8). *How do flat panel detectors work?* Medical Imaging Experts. Retrieved November 11, 2021, from https://www.examvuedigitalxray.com/2019/07/18/how-do-flat-panel-detectors-work/.
5. *Canon Medical Systems USA*. Canon Medical Systems USA, Inc. (n.d.). Retrieved September 28, 2021, from https://us.medical.canon/.
6. DeLorenzo, M. C., & Goode, A. R. (2019, September 30). *Evaluation of skin dose calculation factors in interventional fluoroscopy*. American Association of Physicists in Medicine (AAPM). Retrieved September 28, 2021, from https://aapm.onlinelibrary.wiley.com/doi/pdf/10.1002/acm2.12725.
7. *Evaluation: Toshiba Infinix-I sky angiography system for Interventional Radiology/Vascular Applications*. ECRI. (n.d.). Retrieved September 28,

2021, from https://www.ecri.org/search-results/member-preview/hdjournal/pages/eval-toshiba-infinix-i-sky-angiography-system.

8. Fabjan, C. W. (2004, June 22). *Collider detectors for Multi-tev particles*. Encyclopedia of Physical Science and Technology (Third Edition). Retrieved March 17, 2022, from https://www.sciencedirect.com/science/article/pii/B0122274105001198?via%3Dihub
9. Imaging Technology News. (n.d.). Comparison Chart Compiled by Imaging Technology News. Retrieved January 24, 2022, from https://s3.amazonaws.com/sgcimages/08_09_12_13_IMG_POChart_0316itn.pdf
10. Jones, A. K., & Pasciak, A. S. (2011, November 15). *Calculating the peak skin dose resulting from fluoroscopically guided interventions. part I: Methods*. Journal of applied clinical medical physics. Retrieved September 28, 2021, from https://www.ncbi.nlm.nih.gov/pmc/articles/PMC5718743/.
11. Jones, J. (2013, September 28). *Detective quantum efficiency: Radiology reference article*. Radiopaedia Blog RSS. Retrieved February 16, 2022, from https://radiopaedia.org/articles/detective-quantum-efficiency-1?lang=us
12. Lin P-JP, Goode AR,Corwin FD, et al. AAPM Task Group Report 272:Comprehensive acceptance testing andevaluation of fluoroscopy imaging systems.MedPhys. 2022;1-49.https://doi.org/10.1002/mp.15429 11

13. Lin P-JP, Goode AR. Accuracy of HVL measurements utilizing solid-state detectors for radiography and fluoroscopy X-ray systems. J Appl Clin Med Phys. 2021;22: 339–344. https://doi.org/10.1002/acm2.13389
14. Lin, P.-JP, Schueler+, B. A., Balter, S., Strauss, K. J., Wunderle, K. A., LaFrance, T. M., Kim, D.-S., Behrman, R. H., Shepard, J. S., & Bercha, I. H. (n.d.). *Accuracy and calibration of integrated radiation output indicators in diagnostic radiology: A report of the AAPM Imaging Physics Committee Task Group 190*. Accuracy and calibration of Integrated Radiation Output Indicators in diagnostic radiology: A report of the AAPM Imaging Physics Committee Task Group 190. Retrieved January 21, 2022, from https://aapm.onlinelibrary.wiley.com/doi/epdf/10.1118/1.4934831
15. Lin, P.-J., & Rauch, P. (n.d.). *Functionalityandoperationoffluoroscopic ... - AAPM*. Functionality and Operation of Fluoroscopic Automatic Brightness Control/Automatic Dose Rate Control Logic in Modern Cardiovascular and Interventional Angiography Systems. Retrieved March 22, 2022, from https://aapm.org/pubs/reports/RPT_125.pdf
16. Okuno, E. (n.d.). *Chapter 21: Instrumentation for dosimetry*. Retrieved October 6, 2021, from https://humanhealth.iaea.org/HHW/MedicalPhysics/TheMedicalPhysicist/Studentscorner/HandbookforTeachersandStudents/Chapter_21.pdf.
17. *Philips Allura Xper FD20 Cath/Angio System*. Philips Allura Xper FD20 Cath/Angio System - Avante Health Solutions. (n.d.). Retrieved

September 28, 2021, from https://avantehs.com/p/philips-allura-xper-fd20-cathangio-system/13790.

18. *Scientific, technical publications in the nuclear field | IAEA*. (n.d.). Retrieved March 17, 2022, from https://www-pub.iaea.org/MTCD/Publications/PDF/TRS457_web.pdf
19. *Siemens Artis Zeego Tech Specs (technical ... - UMETEX*. (n.d.). Retrieved September 28, 2021, from https://umetex.ru/wa-data/public/shop/manuals/Siemens-Artis-Zeego-Tech-Specs.pdf.
20. *Part 20—standards for protection against radiation | nrc.gov*. (n.d.). Retrieved March 11, 2022, from https://www.nrc.gov/reading-rm/doc-collections/cfr/part020/full-text.html
21. *Quality and safety - jointcommission.org*. (n.d.). Retrieved March 23, 2022, from https://www.jointcommission.org/-/media/tjc/newsletters/jc-online-july-21-2021.pdf